ELSEVIER

Journal of Materials Processing Technology 100 (2000) 156–162

Journal of Materials Processing Technology

www.elsevier.com/locate/jmatprotec

Simulation of the controlled rolling and accelerated cooling of a bainitic steel using torsion testing

A.B. Cota[a], R. Barbosa[b], D.B. Santos[b,*]

[a]Department of Physics, Federal University of Ouro Preto, Ouro Preto, Minas Gerais, Brazil
[b]Department of Metallurgical and Materials Engineering, Federal University of Minas Gerais, Belo Horizonte, Minas Gerais, Brazil

Received 31 August 1999

Abstract

Controlled rolling, followed by accelerated cooling, was simulated by means of torsion tests. High-strength low-alloy (HSLA) low-carbon (0.08%) bainitic steel containing B, recently developed by the industry as a bainitic steel grade of the API X80 class, was examined. The influence of cooling rate and finish-cooling temperature on the microstructure and mechanical properties were studied. The final microstructure was predominantly bainitic. For a finish-cooling temperature of 400°C the microstructure consists of fine laths of bainitic ferrite with interlath MA constituent, and increase in the cooling rate leads to a continuous increase of the tensile and yield strengths of 158 and 183 MPa, respectively. The analysis of the results enabled the establishment of quantitative relationships between the accelerated cooling variables and the mechanical properties of steel.

Keywords: Torsion testing; Accelerated cooling; Bainitic steel; Mechanical properties

1. Introduction

Recently several investigations have been developed with the objective of studying the influence of the cooling variables (cooling rate and start- and finish-cooling temperatures) on the microstructure and mechanical properties [1–6] of high-strength low-alloy (HSLA) steels, through simulations of rolling and accelerated cooling processes. Such simulations are usually performed by rolling on laboratory or pilots mills and the cooling rates and finish-cooling temperatures after rolling are often difficulties to control.

In an attempt to find an alternative to the conventional approach, a new method based on hot torsion testing to simulate controlled rolling and on gas-accelerated cooling was proposed in the present work. Computerized hot torsion testing is the technique that best simulates industrial rolling [7], enabling a excellent control of the thermo-mechanical processing parameters (temperature, deformation per pass, strain rate and inter-pass time). The use of gas-accelerated cooling also permits an easier and more precise control of the cooling rate and finish-cooling temperature.

This technique was used to study the influence of the cooling rate (Cr) and finish accelerated-cooling temperature (T_{FC}) on the microstructure and mechanical properties of a HSLA low-carbon bainitic steel, recently developed by the metallurgical industry. For the steel investigated the microstructural evolution and the mechanisms for the refinement of the microstructure are discussed. Quantitative relationships between the cooling variables and the mechanical properties of the steel were obtained by means of multiple regression analysis.

2. Experimental procedure

The chemical composition of the steel used in the present investigation is given in Table 1. The steel contains Nb, Ti and V as microalloying elements and B (24 ppm) to enhance hardenability.

Tubular torsion specimens (16.5 mm gauge length, 6.5 mm outer and 2 mm inner diameter) were machined from pieces cut longitudinally along the rolling direction. The hot torsion tests were carried out in a servo-hydraulic torsion machine with a computerized MTS TestStar II™ unit and Testware SX™ software, to control the hydraulic servo-valve and the data acquisition system. A thermo-

* Corresponding author. Tel.: +55-031-238-1803; fax: +55-031-238-1815.
E-mail address: dsantos@demet.ufmg.br (D.B. Santos).

0924-0136/00/$ – see front matter
PII: S0924-0136(99)00467-7

Table 1
Chemical composition of steel (wt.%)

C	Mn	Si	P	Al	Nb	V	Ti	Ni	B	S	N
0.08	1.70	0.25	0.021	0.029	0.033	0.058	0.026	0.17	0.0024	0.002	0.0048

couple was placed inside the specimen and was also connected to an interface card installed in a personal computer, allowing to control the thermal profiles during thermomechanical processing and data collection of the cooling curves.

A simplified controlled rolling schedule was first established based on the knowledge of the non-recrystallization temperature, T_{nr}=970°C. The samples were reheated to 1200°C for 900 s and then cooled down at a rate of 1°C/s. During the cooling they were submitted to nine passes of 20% of equivalent strain each, at a strain rate of 2 s^{-1}. The final pass temperature was chosen as 800°C. Details of the temperature of each pass of the hot torsion experiments are given in Fig. 1.

A CCT diagram of this steel was determined by thermal analysis of the cooling curves from deformed austenite by torsion testing according to the simplified controlled rolling schedule described above. This diagram was used in the selection of the cooling rates and finish-cooling temperatures.

The accelerated-cooling conditions used after the thermomechanical processing are also indicated in Fig. 1. The cooling rates measured correspond to average values for the temperature range of 800–500°C. After the interruption of the accelerated cooling, the samples were cooled down to the room temperature at a rate of 1.0°C/s. To control the cooling rate after deformation a cooling device using helium was developed. This cooling device was composed of a torus with a rectangular cross-section, as illustrated in Fig. 2, similar to that reported by Debray et al. [8]. The cooling rate and the finish-cooling temperature were controlled by means of a panel which permitted close regulation of the helium flow rate, this panel being shown schematically in Fig. 3.

Samples for metallographic observation and Vickers hardness measurements (load of 4.905 N) were sectioned longitudinally producing a tangential plane to the gauge length of the torsion specimens and were prepared according to a standard method. For examination of the microstructure, 2% nital and LePera's etchants [9] were used. The samples were observed by optical and electron scanning microscopy. Volume fraction and dimensions analysis of the constituents were performed using computerized image analysis, IMAGE PRO-PLUS^{TM}, from optical microscopy.

The mechanical properties at room temperature were determined by tensile testing, the tubular torsion specimens being used directly as specimens for tensile testing. The tests were carried out at initial strain rate of 10^{-2} s^{-1} and three tests were performed for each experimental condition of accelerated cooling.

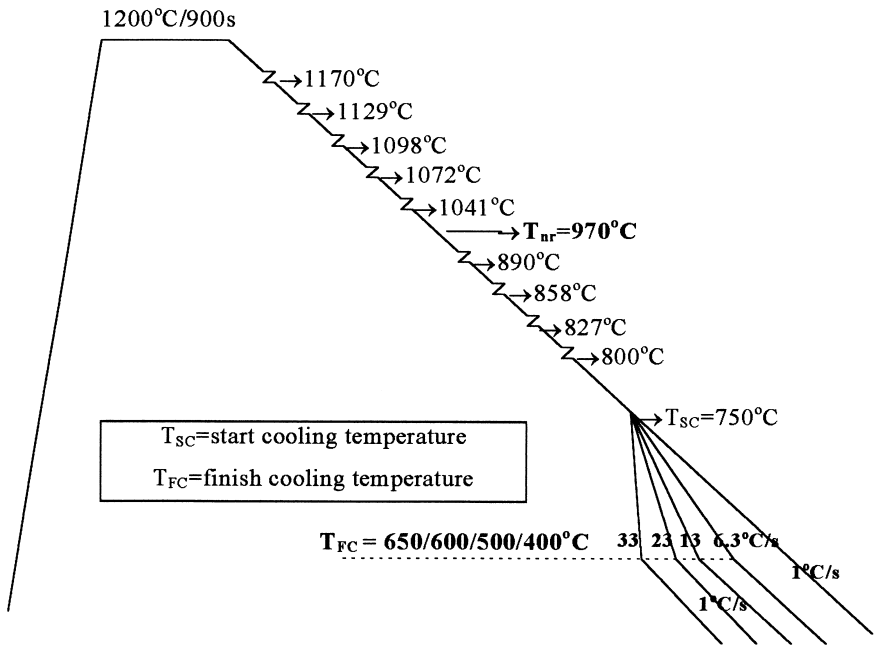

Fig. 1. Schematic representation of the simulation of the controlled rolling and accelerated cooling.

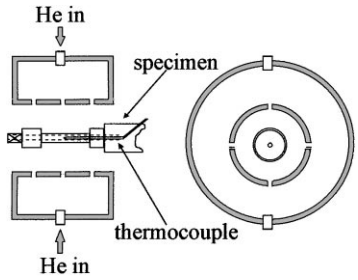

Fig. 2. Cooling device with a specimen in the cooling position.

3. Results and discussion

3.1. CCT diagram

The cooling curves were differentiated with respect to time so to enhance the deviations due to the heat generated whilst the transformation was going on. Prior to differentiation, the experimental scatter inherent to measurements in temperature during cooling was filtered out by a procedure described elsewhere [10]. The start of austenite transformation was measured at a point on a dT/dt versus T curve where there was a deviation from the main curve as indicated by the arrows in Fig. 4. This figure indicates the temperatures for the start and finish of bainite formation, B_S and B_F, respectively. The CCT diagram obtained as described here for the steel of this study is then presented as Fig. 5. The diagram also indicates the cooling rates employed in the experiments as well as the measured values of Vickers hardness. For cooling rates up to 33°C/s the microstructure is predominantly bainitic. This figure shows that increase in the cooling rate causes a decrease in the bainite start transformation temperature, B_S.

3.2. Microstructure

The combined effects of the cooling rate and the finish-cooling temperature on the microstructure are illustrated in Fig. 6 (SEM photomicrographs). For the conditions of thermo-mechanical processing and accelerated cooling used in the present work, the results show that the microstructure

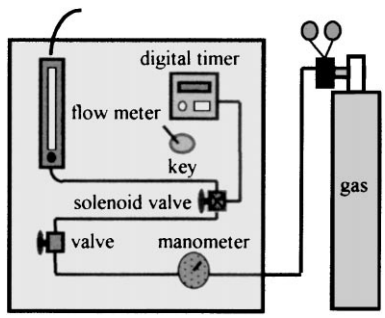

Fig. 3. Schematic illustration of the panel for monitoring and controlling the gas flow.

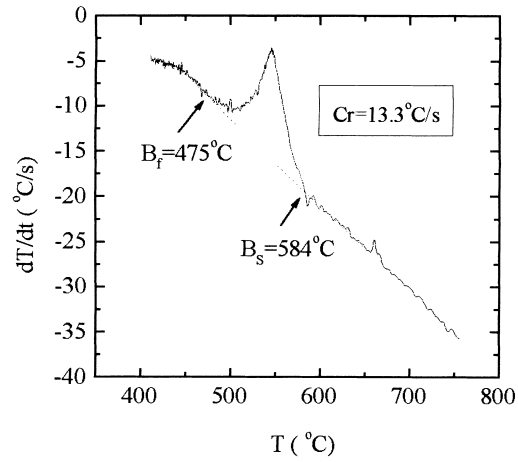

Fig. 4. Cooling rate as a function of the temperature for a rate of 13.3°C/s. The arrows indicate how the B_S and B_F temperatures were measured.

is predominantly bainitic, confirming the effect of boron in increasing the bainitic hardenability. The grain size and volume fraction of ferrite polygonal decreases as the cooling rate is increased or as the finish-cooling temperature is decreased.

It can be seen from Fig. 6a that the microstructure associated with a higher finish-cooling temperature (T_{FC}=650°C) consists of polygonal ferrite (volume fraction ≈12%), granular bainite and small particles of constituent MA, martensite and retained austenite (volume fraction ≈4.5% and particles of average size less than 2 μm), in the bainitic matrix.

By contrast, the microstructure associated with a lower finish-cooling temperature (T_{FC}=500°C), Fig. 6b consists of granular bainite and ferrite bainitic. In this microstructure fine-grained polygonal ferrite can be seen, with small-sized and randomly-distributed MA constituent.

For lower finish-cooling temperatures (T_{FC}=400°C), Fig. 6c–f, the microstructure is essentially bainitic with fine laths

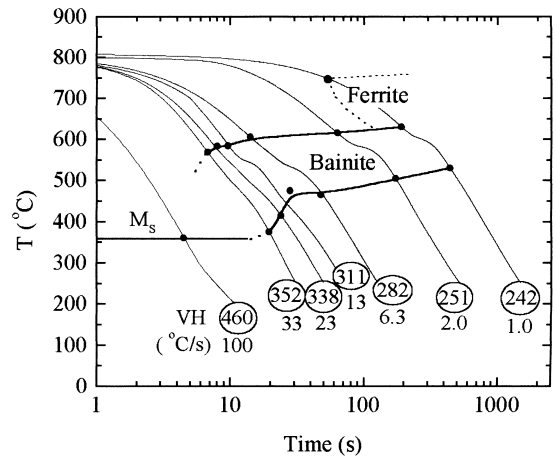

Fig. 5. CCT diagram of a HSLA bainitic steel with thermo-mechanical processing prior to austenite transformation.

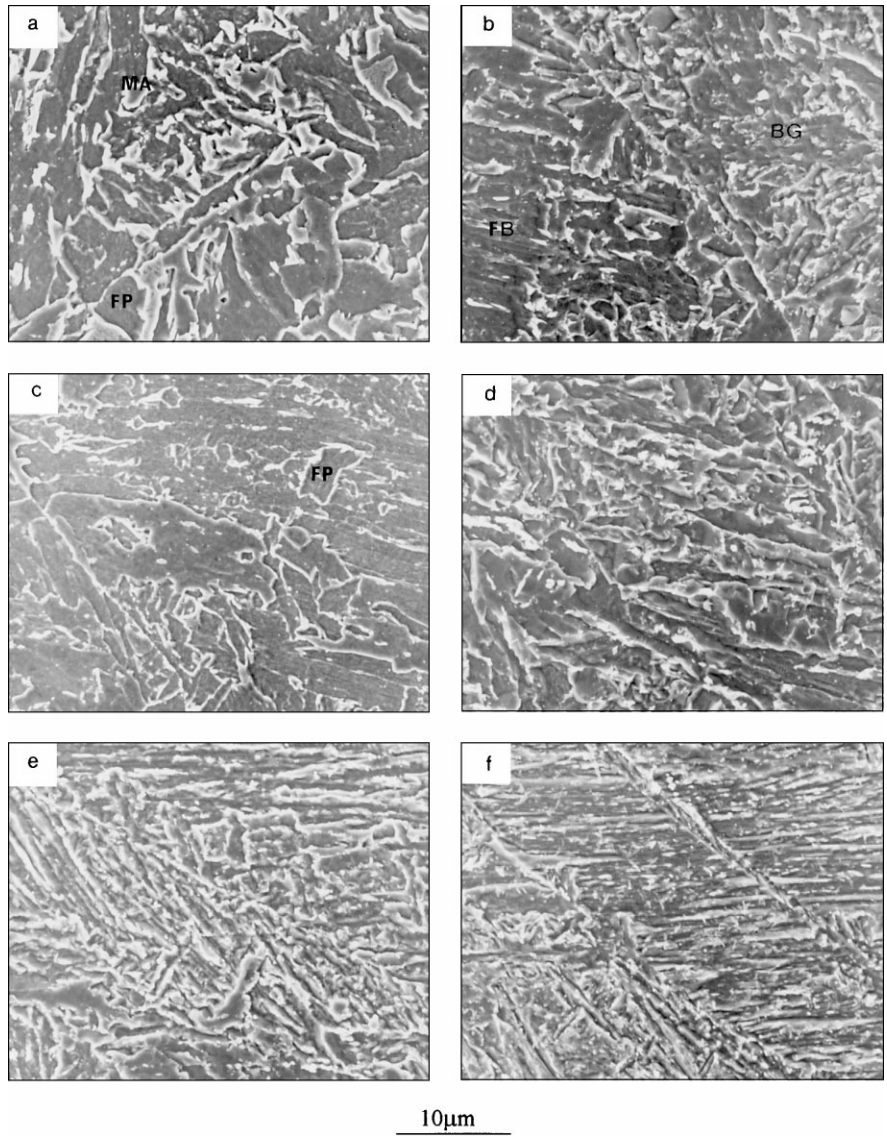

Fig. 6. SEM photomicrographs (2000×) for samples cooled at different rates and finish-cooling temperatures: (a) 6.3°C/s–650°C; (b) 13.3°C/s–500°C; (c) 6.3°C/s–400°C; (d) 13.3°C/s–400°C; (e) 23°C/s–400°C; and (f) 33°C/s–400°C (FP: polygonal ferrite; MA: constituent MA; GB: granular bainite; BF: bainitic ferrite).

of bainitic ferrite with interlath MA constituent. It can be seen in this figure that the width of the bainitic ferrite laths decreases with increase in the cooling rate. The refinement of the bainitic ferrite by the cooling rate could be due to the following: when the cooling rate increases, the reduction in the B_S temperature leads to an increase in the driving force (the difference of the free energy between austenite phase and ferrite phase) for the nucleation rate of sub-units of ferrite and, consequently, to a decreases of the width of bainitic ferrite laths. Increase in the cooling rate leads to a continuous increase of the Vickers hardness from 262 to 320.

In the case of higher finish-cooling temperatures ($T_{FC} \geq 400$°C), the MA constituent islands are distributed almost uniformly throughout the bainitic matrix, Fig. 7a–d. This figure (binary images: MA islands appears white) shows that increase in the cooling rate or decrease in the finish-cooling temperature implies a decreasing in the volume fraction and average size of the MA islands.

3.3. Mechanical properties

Figs. 8–10 show the influence of the cooling rate on the mechanical properties, i.e. the ultimate tensile strength (UTS), yield strength ($\sigma_{0.2}$) and total elongation (El), associated with the various finish-cooling temperatures.

Analyzing Figs. 8 and 9, a tendency is observed for the tensile and yield strengths to increase when the cooling rate increases or when the finish-cooling temperature decreases. The values of these mechanical properties are greater than the corresponding values obtained at a cooling rate of 1°C/s. For finish-cooling temperatures of 650–600°C, the influence of the cooling rate was not significant. The variations in

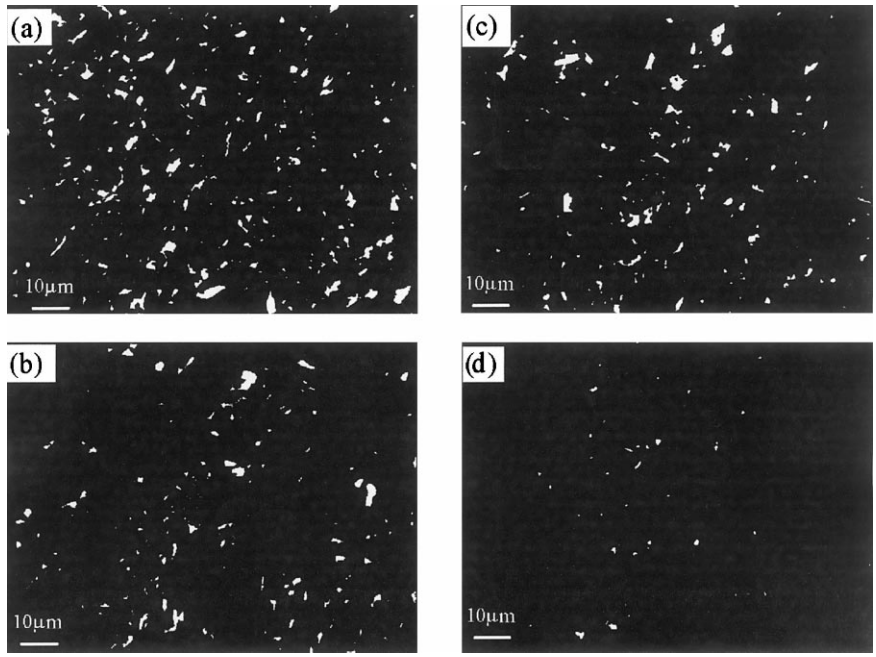

Fig. 7. Binary images (1000×) for samples cooled at different rates and finish-cooling temperatures: (a) 6.3°C/s–650°C; (b) 33.0°C/s–650°C; (c) 13.3°C/s–650°C; and (d) 13.3°C/s–500°C (LePera's etchant: constituent MA is white).

these properties were qualitatively consistent with the changes in microstructure induced by the variations in the accelerated-cooling conditions.

For the finish-cooling temperature of 400°C, the cooling rate has a strong influence on the tensile and yield strengths, as shown in Figs. 8 and 9. Increase in the cooling rate lead to a continuous increase of the tensile and yield strengths of 748–906 MPa and 660–843 MPa, respectively. Results from the literature [11–13] show that the width of the bainitic ferrite laths decreases and the dislocation density increases with decrease in the B_S temperature. Therefore, when the cooling rate increases, the reduction in the B_S temperature leads to an increase in the tensile and yield strengths.

The yield ratio ($\sigma_{0.2}$/UTS) varied from 0.75 (Cr=6.3°C/s–T_{FC}=650°C) to 0.93 (Cr=33°C/s–T_{FC}=400°C). The tendency of the yield strength to increase with increase of the cooling rate is a consequence of the interruption of the accelerated cooling at temperatures greater than or equal to 400°C, which prevented the formation of martensite.

Tubular specimens and standardized specimens to the ASTM A370-89 [14] specification were machined from material as received from the industry. The total elongation measured in the tensile testing were of 35.2 and 23.9% for the tubular and standard specimens, respectively. The elongation values presented in Fig. 10 were then corrected by multiplication by a factor of 0.68 (=23.9/35.2). This figure

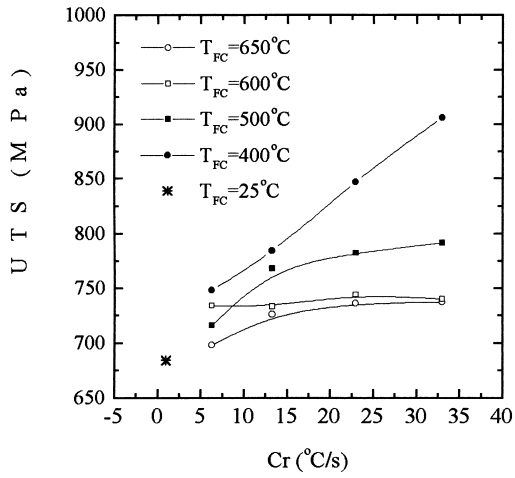

Fig. 8. Influence of the cooling rate (Cr) on the UTS (ultimate tensile strength).

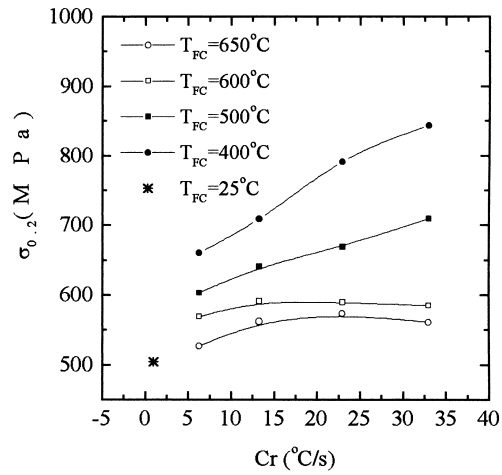

Fig. 9. Influence of the cooling rate (Cr) on the $\sigma_{0.2}$ (yield strength).

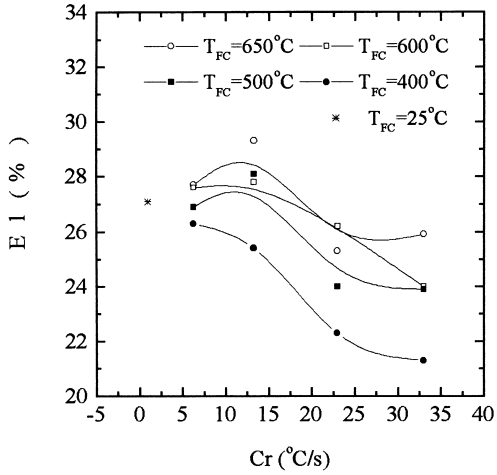

Fig. 10. Influence of the cooling rate (Cr) on the El (total elongation).

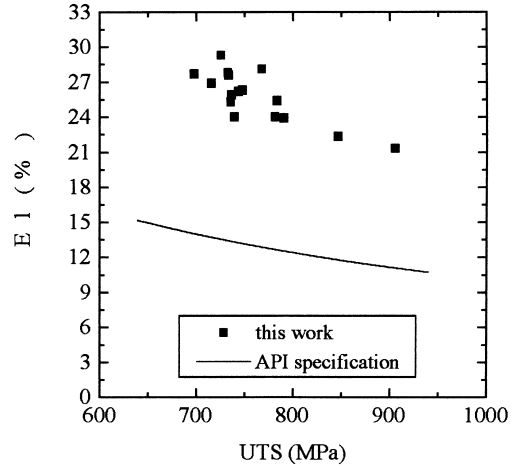

Fig. 11. Correlation between the elongation total and tensile strength [15].

shows a tendency of decrease of the total elongation when the cooling rate increases or the finish-cooling temperature decreases. This result is in agreement with those from the literature [2–5,11–13] for HSLA low-carbon bainitic steels, which show a decrease in the total elongation when the tensile strength increases.

From the practical standpoint, moreover, it would be useful to determine simple equations expressing the relationships between the cooling variables and the performance of the steel. A statistical treatment of the data obtained in the present work was then undertaken. This treatment was carried out by taking the cooling rate and finish-cooling temperature as independent variables. Multiple regression equations were established using the step-wise method.

The mechanical properties (MP) are considered to be defined as the sum of the mechanical properties of air-cooled steel under corresponding thermo-mechanical processing conditions (MP_{AC}) and an increment of mechanical properties by accelerated cooling (ΔMP). The value (MP_{AC}) is a function of the chemical composition of the steel and of the thermo-mechanical processing

$$MP = \Delta MP + MP_{AC}. \quad (1)$$

The following equations were obtained:

$$\Delta UTS\ (\pm 30\,MPa) = 33.6 + 14.2Cr - 0.022Cr T_{FC},\quad R = 96.5\%, \quad (2)$$

$$\Delta\sigma_{0.2}\ (\pm 42\,MPa) = 73.5 + 23.5Cr - 0.038Cr T_{FC},\quad R = 97.6\%, \quad (3)$$

$$\Delta El\ (\pm 2\%) = 1.5 - 0.46Cr + 5.8 \times 10^{-4} Cr T_{FC},\quad R = 90.3\%, \quad (4)$$

where Cr is the cooling rate in °C/s, T_{FC} the finish-cooling temperature in °C, R the multiple correlation coefficient and ΔUTS, $\Delta\sigma_{0.2}$, ΔEl, are the increment of tensile strength, yield strength and total elongation by accelerated cooling, respectively. The values enclosed within the brackets indicate 95% confidence level.

Figs. 8–10 and Eqs. (2)–(4) show that the mechanical strength is more affected by the finish-cooling temperature, whereas the total elongation is more influenced by the cooling rate.

The regression equations relating the cooling rate and the finish-cooling temperature to the mechanical properties indicate that the best combination of ductility (El=28.1%) and tensile strength (UTS=768 MPa) is obtained with Cr=13.3°C/s and T_{FC}=500°C. Results from the literature [1–5] also indicate the temperature of 500°C as the best finish-cooling temperature for a great variety of steel grades, although there is no quantification relating the mechanical properties and the processing variables. Under these cooling conditions, the microstructure (Fig. 6b) is essentially bainitic (bainitic ferrite and granular bainite) with 7.0% of polygonal ferrite and MA constituent (≈1.0% and an average size of 1.0 μm).

The minimum requirement for total elongation (El) according to the API specification [15] for specimens with 50 mm gauge length is given by

$$El\ (\%) = 1943.95 \frac{A^{0.2}}{UTS^{0.9}}, \quad (5)$$

where A is the cross-sectional area of the specimen in mm^2 and UTS is in MPa. In Fig. 11, all of the results are given as a correlation between tensile strength and total elongation for specimens with a diameter of 12.5 mm. As seen, all of the measured elongation values fulfill the API specification.

4. Conclusions

The phase transformation behavior of the steel under investigation, expressed in terms of the CCT diagram, was used in the selection of the cooling rates and finish-cooling temperatures to be adopted during thermo-mechan-

ical processing, aiming at avoiding the formation of martensite and optimizing the mechanical properties. The results of the simulations of controlled rolling and accelerated cooling by means of the torsion testing of samples of HSLA bainitic steel are presented.

The analysis of the regression equations determined in the present investigation indicated that the best combination of ductility and tensile strength is obtained with Cr=13.3°C/s and T_{FC}=500°C.

For the conditions of thermo-mechanical processing and accelerated cooling used in this work, the results show that microstructure is predominantly bainitic, confirming the boron effect in increasing the bainitic hardenability. The results show that increase in the cooling rate or decrease in the finish-cooling temperature implies a decreasing in the volume fraction and average size of the MA islands and of the polygonal ferrite. For T_{FC}=400°C the microstructure is essentially bainitic with fine laths of bainitic ferrite with interlath MA constituent.

The yield strength of 550 MPa, at the tensile strength of 700 MPa and the minimum requirement of total elongation for the grade API X80 were found in the samples for all of the cooling conditions.

Acknowledgements

The authors are grateful for the financial support of CNPq and FAPEMIG. The authors also thank Usiminas for supplying the material used in this work.

References

[1] K. Amano et al., in: G.E. Ruddle, A.F. Crawley (Eds.), Proceedings of the Accelerated Cooling of Rolled Steel, Pergamon Press, Winnipeg, 1987, pp. 43–56.
[2] P. Bufalini et al., in: P.D. Southwick (Ed.), Proceedings of the Accelerated Cooling of Steels, The TMS of AIME, Pittsburgh, 1985, pp. 387–400.
[3] L.E. Collins et al., in: G.E. Ruddle, A.F. Crawley (Eds.), Proceedings of the Accelerated Cooling of Rolled Steels, Pergamon Press, Winnipeg, 1987, pp. 57–70.
[4] M. Pontremoli et al., Met. Technol. 11 (1984) 504–514.
[5] C. Shiga et al., in: M. Korchynsk (Ed.), Proceedings of the Conference on Technology and Applications of HSLA Steels, ASM, Metals Park, Philadelphia, 1983, pp. 643–654.
[6] P.C. Rodrigues, A.B. Cota, D.B. Santos, in: T. Chandra, T. Sakai (Eds.), Proceedings of the International Conference on Thermomechanical Processing of Steel and Other Materials, THERMEC'97, The Minerals, Metals and Materials Society, Wollongong, 1997, pp. 787–792.
[7] L.P. Karjalainen et al., ISIJ Int. 35 (1995) 1523–1531.
[8] B. Debray, P. Teracher, J.J. Jonas, Metall. Mater. Trans. A 26 (1995) 99–111.
[9] F.S. LePera, J. Met. March (1980) 38–39.
[10] P.J. Modenesi, C.L. de Araújo, J.H. Nixon, in: Proceedings of the International Conference on Computerization of Welding Information IV, Orlando, AWS, 1992.
[11] M. Katsumata et al., Mater. Trans. 32 (1991) 715–728.
[12] C.I. Garcia et al., ISS Trans. 13 (1992) 103–112.
[13] F.B. Pickering, Physical Metallurgy and Design of Steels, Applied Science Publishers, London, 1978, p. 101.
[14] American Society for Testing and Materials, Standard test methods and definitions for mechanical testing of the products, A 370-88, Annual Book of Standards, Philadelphia, 1988, pp. 37–43.
[15] API Specification 5L for Line Pipe, 41st Edition, April 1995, p. 6.